Hindawi
Advances in Civil Engineering
Volume 2018, Article ID 5474165, 12 pages
https://doi.org/10.1155/2018/5474165

Research Article

Study on Fracture and Stress Evolution Characteristics of Ultra-Thick Hard Sandstone Roof in the Fully Mechanized Mining Face with Large Mining Height: A Case Study of Xiaojihan Coal Mine in Western China

Feng Ju, Meng Xiao, Zequan He, Pai Ning, and Peng Huang

State Key Laboratory for Geomechanics and Deep Underground Engineering, China University of Mining & Technology, Xuzhou 221116, China

Correspondence should be addressed to Feng Ju; juf1983@163.com and Meng Xiao; xiao_meng1993@126.com

Received 30 August 2018; Accepted 10 October 2018; Published 13 November 2018

Guest Editor: Dengke Wang

Ultra-thick hard sandstone roofs present high thickness, poor delamination, and wide caving range. The strata pressure of the working face during actual mining increases, having a significant influence on the safe mining of the working face. Especially, in the mining areas of western China, the fully mechanized mining faces with high mining height and high-strength mining are more prominent. Understanding the fractures and stress evolution characteristics of the ultra-thick hard sandstone roof during actual mining is of high significance to control the dynamic pressure on the working face. In this paper, the typical ultra-thick hard sandstone roof of the Xiaojihan coal mine was taken as an example. The structural and chemical composition characteristics were analyzed. Besides, the fracture characteristics of ultra-thick hard roof during the working face mining were analyzed. Moreover, the fracture structure consistency was verified through physical simulation and a field measurement method. Finally, the stress evolution laws in the ultra-thick hard sandstone roof fracture were studied through numerical simulation. The findings demonstrated that (1) the ultra-thick hard sandstone roof was composed of inlaid coarse minerals, which had compact structure, while the Protodyakonov hardness reached up to 3.07; (2) under the high-strength mining condition of fully mechanized mining face with large mining height, the ultra-thick hard sandstone roof had the characteristics of brittle fracture, with a caving span of 12 m; (3) under the high-strength mining condition of fully mechanized mining face with large mining height, the ultra-thick hard sandstone roof followed the stress evolution laws that were more sensitive to the neighboring goaf. Therefore, it was necessary to reduce the fracture span or layering of ultra-thick hard sandstone roof through the manual intervention method adoption or increase either the strength of coal pillar or supporting body, to resist the impact generated during ultra-thick hard sandstone roof fracture.

1. Introduction

Coal still constitutes the main fossil fuel for energy production throughout the world. To reduce the index of death rate per million-ton coal (DRPMT) in coal mines, the goal achievement of a highly intensive production of modern coal mines is an important approach. At present, coal mines, both domestically and abroad, have been developed as large-scale modern mines, with a capacity of tens of millions of tons, in the mode of "one mine, one face." In China, up to 36 pairs of mines exist, of tens of millions tons in capacity, while 34 pairs are under construction or being expanded. Most of these mines are distributed in the mining areas within western China, demonstrating the characteristics of high-intensive mining, such as having working faces with large mining height, high advance speed, and long advance distance [1]. Ultra-thick hard sandstone roof is a certain geological condition, recently discovered but commonly found during the high-intensive coal mining in western China. This type of roof has several characteristics, such as

high strength, high elastic modulus, undeveloped joint fissures, high thickness, strong wholeness, and strong self-bearing capacity. Following coal mining, the roofs move and sustain fracture, easily leading to stress concentration, consequently causing strata behaviors, such as rib spalling, severe deformation of tunnels, and abrupt increase of support loading. Instantaneous caving of large areas of roofs and roof weights severely threatens the production safety in mines [2–5]. Large-scale coal bases in China are the northeastern China, the north of Shanxi Province, the east of Shanxi Province, the central part of Shanxi, the central part of Hebei Province, the southwest of Shandong Province, Huainan and Huaibei, Shendong, the north of Shaanxi, Ningdong, Yunnan and Guizhou, as well as the west of Henan Province. In the mining areas of Yulin, located at the north of Shaanxi, Datong and Yangfangkou in the north of Shanxi, Zaozhuang of Shandong province, Tonghua, Hegang, and Qitaihe in northeast of China, and Jingyuan of Huanglong [6–11], the problems regarding hard roofs are ubiquitous, among which, the accidents of roof falls account for approximately 70% of the accidents on the working faces. The thick hard roof constitutes the root cause of strong mine pressure. The mechanical properties of this type of roof as well as the movement, deformation, damage, and fracture during the working face mining determine the rock pressure and sphere of influence for the entire stope. Therefore, studying the fracture characteristics and stress evolution laws of these roof conditions, during the high-strength mining of fully mechanized mining face with large mining height, is of high significance to control the mine pressure on the working face and guarantee the production safety on the working face.

Many studies on ultra-thick hard sandstone roof mining exist both domestically and abroad. With focus on the fracture mechanism of ultra-thick hard sandstone roof, Wang [12] analyzed the instability mechanism of thick hard roof in Tashan coal mine through the "key strata" theory, while proposing the relationship between roof fracture and abnormal gas emission at the working face. Besides, the Reissner thick plate theory, the Vlasov plate theory [13], and the long-beam theory [14] are often used to analyze the initial and periodic fracture laws of the ultra-thick hard roof. Relevant research techniques mainly include similar simulation, numerical simulation [15], microseismic monitoring, and other methods. Wu [16] successfully analyzed the variation of strata behavior and fissure zone development height in the stope prior to and following ultra-thick hard roof fracture through the physical similar simulation method. Lu [17, 18] analyzed the change law of microseismic signals on the working face coal body prior to and following ultra-thick hard roof fracture, which constituted important reference data for the fracture monitoring of ultra-thick hard roof. Yu [19] and Xu [20] obtained similar conclusions through numerical simulations. The simulation results demonstrated that, when approximately 350 m of working face was mined, full mining was achieved, while severe strata behaviors often appeared. In the aspect of processing method for ultra-thick hard roof, the most commonly used methods are the blasting method and the fracturing method. Guo [8] and Ning [10] successfully solved the problem of severe strata behaviors, caused by ultra-thick hard roofs, through the decompression blasting and deep-hole presplitting blasting methods, respectively. He [21] and Zheng [22] relieved the early-warning of high strata pressure on the working face, guaranteeing safe mining at the working face through the hydrofracturing and sleeve fracturing methods, respectively. Scholars, both domestically and abroad, conducted research on hard roofs, mostly from the perspectives of mine pressure model, energy aggregation, and rock strata movement, through the methods of numerical simulation and theoretical analysis. However, insignificant attention was paid to the fracture and stress evolution characteristics of ultra-thick roofs under high-intensive mining. In this paper, through the 11215 fully-mechanized mining face in the Xiaojihan coal mine consideration as an example, the roof fracture and stress evolution characteristics during mining in the fully-mechanized mining face, under the condition that the ultra-thick sandstone roof was near goaf, were revealed through the methods of theoretical analysis, similar simulation, numerical simulation, and field measurement. This provided the important theoretical basis for the overlying strata control and roadway support at the working face under this condition.

2. General Situation of Engineering

2.1. Layout of Working Face. The Xiaojihan coal mine was located approximately 20 km northwest of Yulin. The mine field was bounded by the north boundary of the Yuheng mine area in the north, adjacent to the Xihongdun and Hongshixia mine fields in the south, as well as connected to Kekegai exploration area in the west and bounded by the Yuxi River in east. The 11215 working face was located in panel 11 of 2# coal bed in the well field, laid out along the coal bed in an inclined manner, with a strike length of 4888 m, an inclined length of 280 m and a mining area of 585600 m^2. At the present stage, the 11213 working face mining ended and in the 11215 working face the mine reached the open-off cut position and goaf for the 11213 working face. The mining of the 11215 working face and its layout are presented in Figure 1.

The 11215 working face mining had entered Area II. A 20 m-section coal pillar was laid out between the 11213 working face and the 11215 working area, when the surrounding rock on the air return way of 11215 working face sustained severe deformation. Rib spalling and deformation of hydraulic single prop occurred, which severely affected the normal production. The cross section of the air return way for 11215 working face was rectangular, with a sectional area of 3.8 × 5.5 m. The roadway excavation was conducted along the bottom plate, with solid coal on one side and coal pillar on the other side.

2.2. Occurrence of Coal-Series Strata. At the present stage, the Xiaojihan coal mining was mainly focused on 2# coal, for which the depth of the coal bed in the 11215 working face was 173.98–460.36 m. The coal bed pitch was 1°~3°, the coal

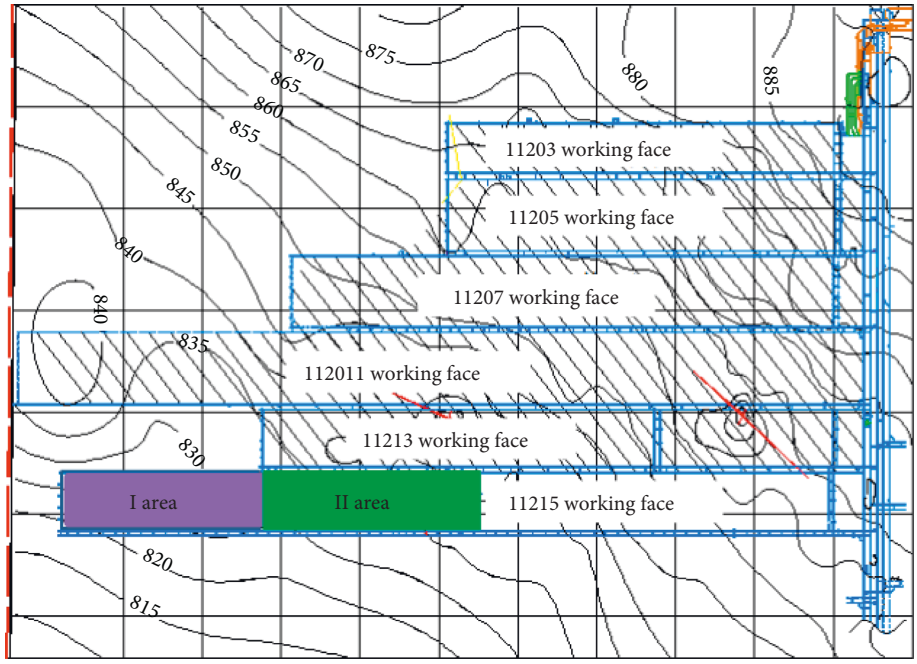

Figure 1: Mining engineering plane diagram.

bed thickness was 3.25~5.04 m, and the average mining height for the coal bed was 4.56 m. The working face mining was conducted through the large-mining-height long wall backward caving method. In the advancing direction of the 11215 working face, the drilling-hole detection was conducted and the geology columnar section of the working face was obtained through analysis, as presented in Figure 2.

It could be observed from the geology columnar section that the immediate roof was medium sandstone, of 6.5 m in average thickness, with a color of gray white and a layered distribution. The internal minerals presented angular shape of dark color, displaying poorer sorting characteristics. The main roof was divided into three parts: the lower part was medium sandstone, the upper part was stratified siltstone, and the middle part was stratified sandstone grit. The main roof presented approximately horizontal layered distribution, with relatively high thickness, high strength, and good stability. This led to difficult fracture occurrence. Most districts of the coal seam floor were mudstone with relatively low strength, which was easy to generate heaving floor. Through the entire borehole columnar section analysis, it could be observed that the roof of 11215 working face belonged to interbedding of sandstone and mudstone, in which, the sandstone accounted for a high proportion. The cumulative proportion of sandstone over 5 m of thickness for a single layer exceeded 58.2%, and the cumulative proportion of sandstone over 10 m of thickness exceeded 38.9%. It could be considered that the entire roof of the working face was dominated by relatively intact sandstone, while the main roof was felspar sandstone stratum of 19.79 m (ultra-thick sandstone of nearly 20 m).

2.3. Structure and Mechanical Characteristics of Ultra-Thick Sandstone Roof. The density of the rock sample for the thick sandstone roof was analyzed through SEM (scanning electron microscope). The SEM pictures of the main roof under conditions of different resolutions are presented in Figure 3.

It could be observed that the coarse-grained minerals inside the sandstone roof mostly followed an inlaid distribution mode. The grains were high-sized with high crystallization. The structure was significantly dense, and the pores were not developed.

Through physical mechanics testing on the rock sample for the sandstone roof, its physical mechanics parameters were obtained, as presented in Table 1.

3. Assumption of Ultra-Thick Sandstone Hard Roof Fracture

Figure 4 shows the difference of pressure distribution between complete and layered roof caving. Comparing roof layered caving, the stress above roadway that has ultra-thick roof is much higher, which causes the surrounding rock have large deformation. When the 11215 working face mining progressed to the position of open-off cut of 11213 working face (entering the influence sphere of the goaf for 11213 working face), the goafs of 11215 and 11213 working faces contact interconnected. At this time, the structures of the stope roofs for the two working faces formed the "L-shaped" space structure of the overlying rock with the bearing point being in the goaf area and fracturing lines being in the side of solid coal, as presented in Figure 5. It could be observed that blue lines (inside the solid coal) denoted the fracturing lines of roofs, while the red lines (in the goaf) denoted the lines formed through the bearing point connections of roof fracturing in the goaf. Figure 6 presents the caving state of the suspended roof in the goaf of the 11213 working face

Thickness (m)	Columnar	Key bed	Rock name	Description of the rock
10.87			Feldspar sandstoner	Gray-white block medium feldspar sandstone. Medium sorting, staggered bedding, roundness is sub-angular, obvious pore contact.
1.22		1# coal		Black semi-bright coal. Dark brown streaks, asphalt luster, stepped fractures, brittleness, medium hardness, strip-like structure, layered structure. The coal and rock components are mainly bright coal, followed by dark coal, and a small amount is mirror coal and silk coal. The coal seam is in obvious contact with the top and bottom plates.
6.07			Siltstone	Light gray thick layered siltstone; horizontal bedding; obvious contact with the lower layer.
19.79			Feldspar sandstoner	Gray-white block medium feldspar sandstone. Medium sorting, staggered bedding, roundness is sub-angular, porous mud cementation, obvious contact with the lower layer.
6.53			Feldspar sandstoner	Gray-white block fine feldspar sandstone. Medium sorting, staggered bedding, roundness is sub-circular, porous mud cementation, obvious contact with the lower layer.
0.53			Silty mudstone	Dark gray medium thick layered silty mudstone; horizontal bedding; obvious contact with the lower layer.
5.10		2# coal		Black semi-bright coal. Dark brown streaks, asphalt luster, stepped fractures, brittleness, medium hardness, strip-like structure, layered structure. The coal and rock components are mainly bright coal, followed by dark coal, and a small amount is mirror coal and silk coal. The coal seam is in obvious contact with the top and bottom plates.
3.04			Silty mudstone	Dark gray medium thick layered silty mudstone; horizontal bedding; obvious contact with the lower layer.
11.26			Feldspar sandstoner	Gray-white block fine feldspar sandstone. Medium sorting, staggered bedding, roundness is sub-circular, porous mud cementation, obvious contact with the lower layer.

Figure 2: Composite borehole columnar section for 11215 working face.

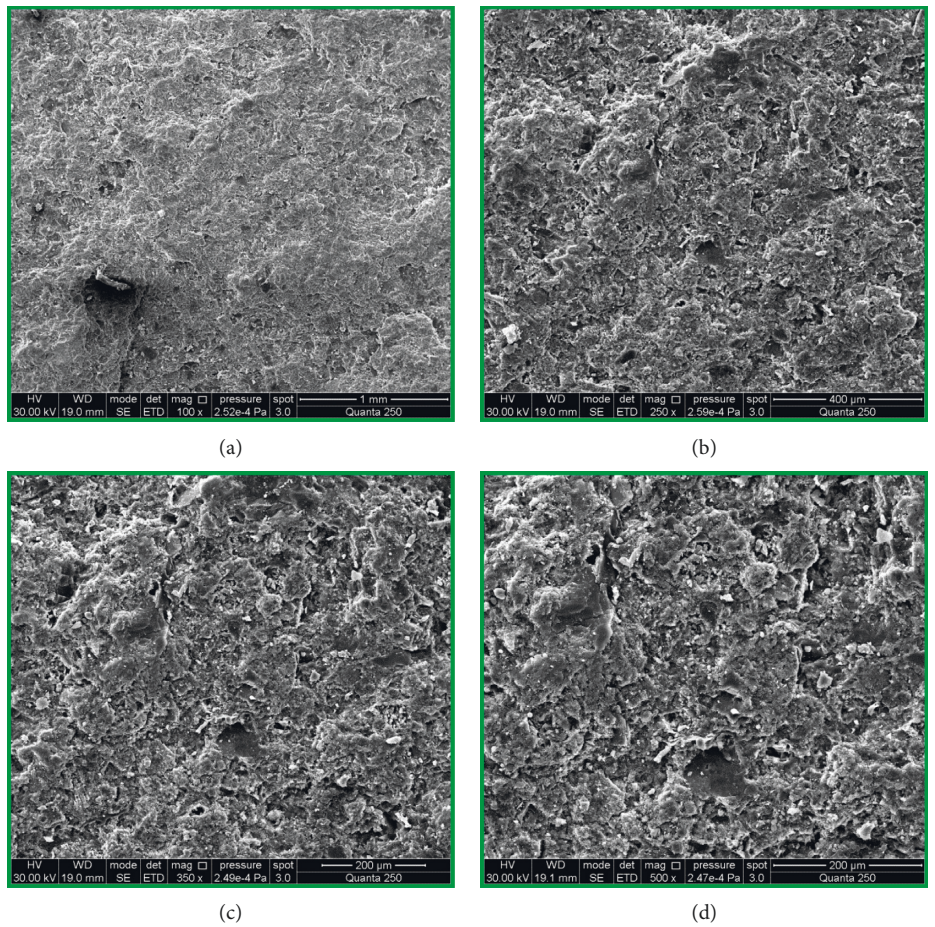

Figure 3: Continued.

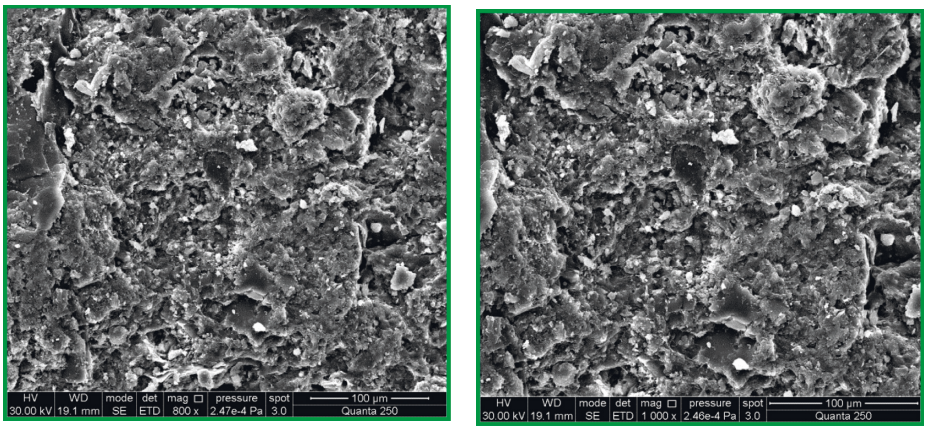

(e) (f)

Figure 3: SEM images at different resolutions in the main roof: (a) 100X; (b) 250X; (c) 350X; (d) 500X; (e) 800X; (f) 1000X.

Table 1: Physical and mechanical parameters of extra-thick sandstone roof.

Item	Density (kg·m^{-3})	Broken expand coefficient	Strength (MPa)			Frictional angle (°)
			Compression	Tensile	Cohesive	
Parameters	2566	1.440	30.67	4.93	7.90	31.04

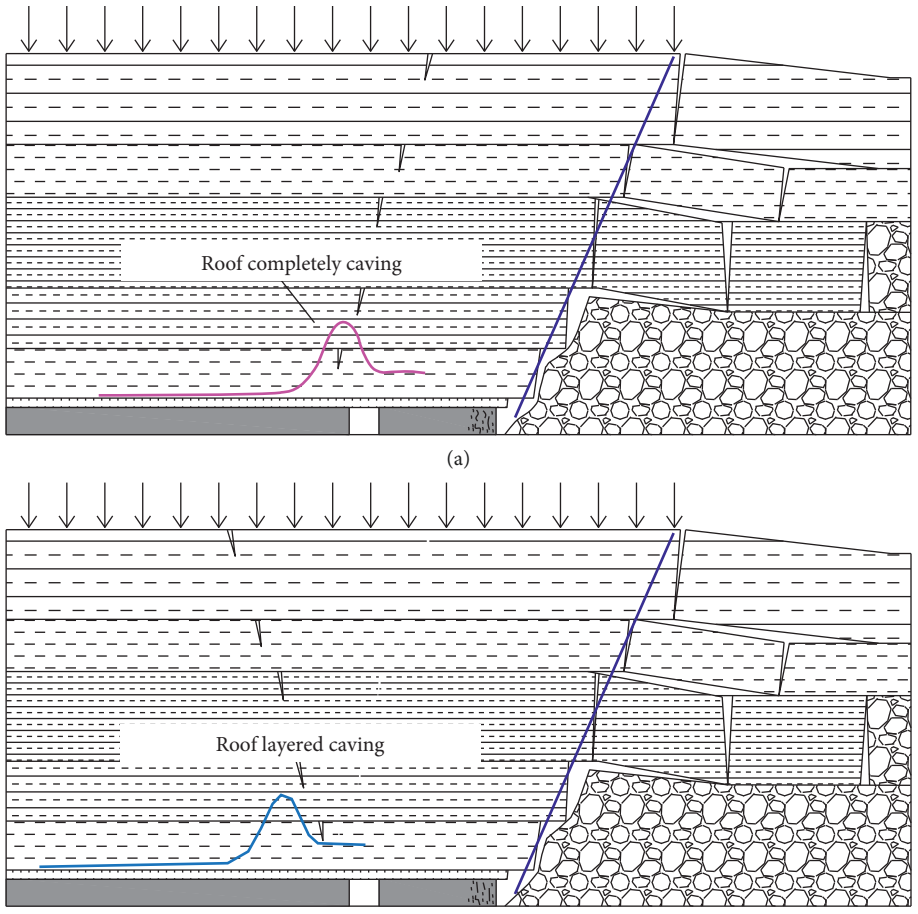

(a)

(b)

Figure 4: Lateral support pressure distribution of coal seam under different roof caving forms: (a) roof completely caving; (b) roof layered caving.

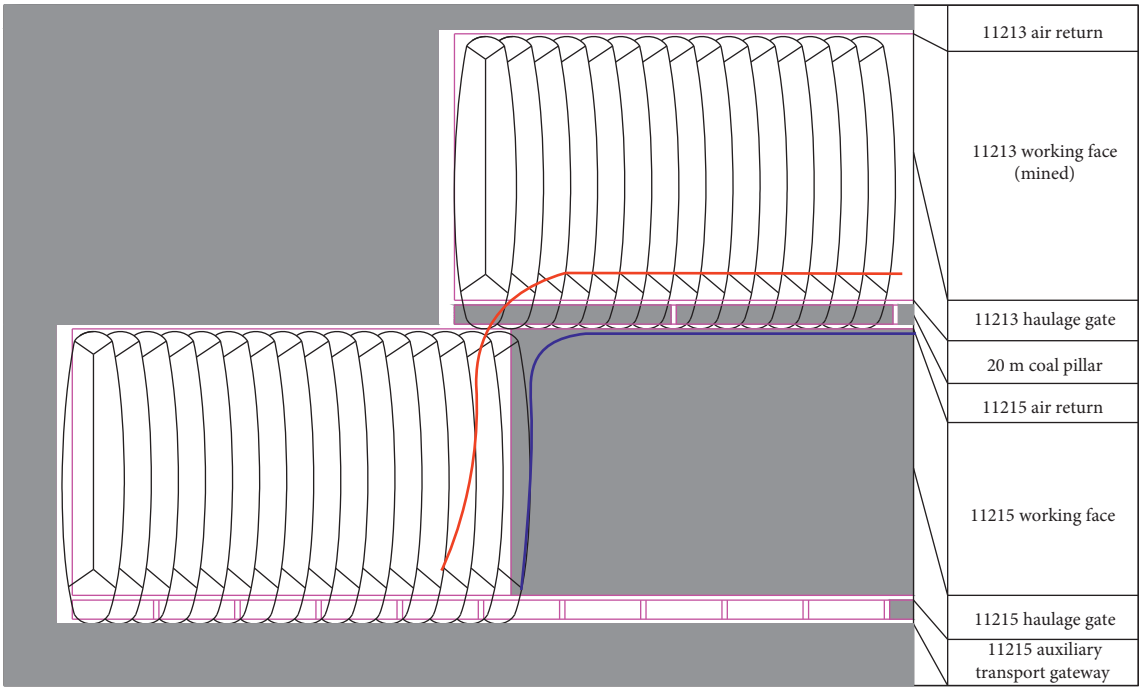

Figure 5: "L-shaped" overlying rock space structure.

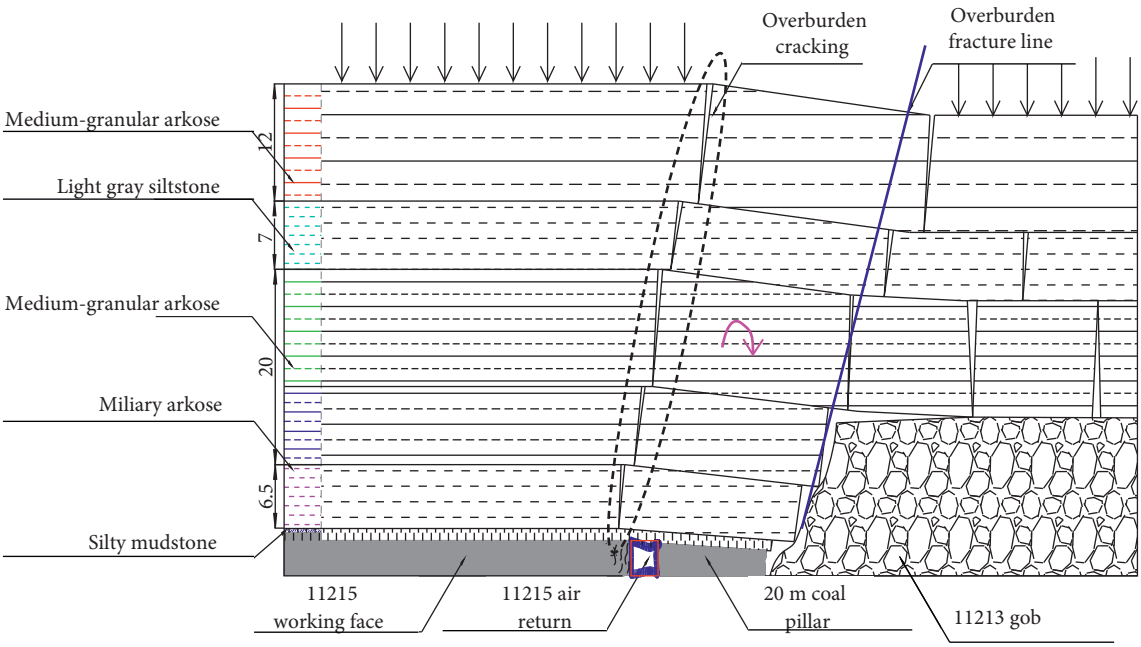

Figure 6: Suspended roof structure of the No. 11213 goaf affected by mining of No. 11215 face.

subsequently to being affected by the 11215 working face mining.

It could be observed from the morphological characteristics of the "L-shaped" space structure of the overlying-rock that the stress above the structure transferred to solid coal and the gangue at the goaf through supporting point. Thereby, two areas of stress concentration formed in both the goaf and solid coal sides. The "L-shaped" space structure of the overlying rock could be interpreted as overlying-rock structures in two working faces cooperatively moving in crosswise dimension, forming high pressure arch, with the inclined arch front and back feet being at a certain area of this working face and the upper working face. In vertical dimension, the balanced structure developed upwards, below which, was fracturing articulated structure. Periodic fracture of the rock strata generated characteristics of periodic pressure appearance. The high rock stratum on the balanced structure transferred gravity stress to the gangue in

the goaf and the solid coal in working face, through layer-by-layer transmission. The instability of the balanced structure would cause dynamic pressure.

When the 11215 working face mining was conducted near the open-off cut position of the 11213 working face, the synergic movement of overlying rocks in the two working faces led to the "L-shaped" space structure formation, causing stress concentration to form above the 20 m isolated coal pillar set in-between the working faces. Therefore, severe surrounding rock deformation and dynamic pressure phenomenon occurred at the end of the 11215 working face and return air roadway. The roof above the coal pillar rotated to the goaf of the 11213 working face, causing deformation of nonproduction side (coal pillar side) on the air return roadway of 11215 working face to far exceed the production side (solid coal side).

The position calculation of the fracturing line on the roof in the goaf of the 11213 working face was of high significance to determine the rational coal pillar width, isolate synergic movement of overlying rocks on the neighboring goafs, and control the roof weighting. The position of fracturing line for the main roof in the working face could be obtained through the elastic foundation beam model. Through the stress conditions on the fractured roof strata, the model could be simplified into the "cantilever-simply support" beam structure in the direction along working face, as presented in Figure 7.

The fractured rock length L_x can be calculated through the following equation on the key strata theory basis:

$$L_x = \frac{\tan^{-1}\left[\left(\beta\left(2\alpha M_0 s + rQ_0\right)\right)/\left(r^2 M_0 + \alpha r Q_0\right)\right]}{\beta}, \quad (1)$$

where

$$\begin{aligned} Q_0 &= q_c L + Q - F, \\ M_0 &= \frac{q_c}{2}L^2 + QL + N\frac{h}{2} - FZ, \\ N &= \frac{LQ}{2\left(h - \Delta s\right)}q_c L, \\ Q &= q_c L, \\ \Delta s &= \frac{h}{6}, \\ s &= \frac{N}{EI}, \\ r^2 &= \frac{k}{EI}, \end{aligned} \quad (2)$$

where α approximately equals to β, the corresponding value can be taken as $0.09\,\mathrm{m}^{-1}$; Q_c presents the uniformly distributed load imposed by the weight of main roof and its upper bearing strata (8 times the mining height); h denotes thickness of the main roof, which was 20 m; k denotes elastic foundation coefficient, of 500 MPa in value; E denotes the elastic modulus of the main roof, of 55 GPa in value; I denotes inertia moment for section of the main roof; F denotes supporting force of the coal pillar; Z denotes the apex distance from the action point of supporting force of the coal pillar to the fixed end; and L denotes the original cantilever length in the main roof. According to the ultimate span equation for the mechanical model of the simply supported beam for the main roof,

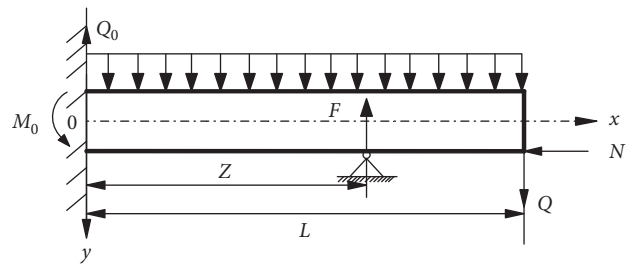

Figure 7: Mechanical model of main roof suspension above coal pillar after mining face.

$$L = 2h\sqrt{\frac{R_T}{3q}}, \quad (3)$$

where h denotes the main roof thickness, which is 20 m; R_T denotes the rock tensile strength of 5.96 MPa; q denotes the uniformly distributed load, which is 8 times the mining height, $q = 0.9$ MPa.

The hanging arch length of the main roof for the 11213 working face under the condition of ultra-thick sandstone can be calculated as 59.4 m.

It was discovered through data statistics that, as the supporting force of coal pillar F gradually increased, L_x gradually decreased, signifying that the higher the supporting force of coal pillar to the main roof was, the shorter the fracturing length of the main top was. Supposing the ultimate limit state, the supporting force of coal pillar to the main roof was 0; consequently, the fracturing length of the main top as maximum. Through calculations, it could be obtained that $L_x(\max) = 43.5$ m.

From Figure 8, the fracturing length of the main top is

$$L_x = L_1 + L_2 + L_3, \quad (4)$$

where L_1 denotes the suspension length of the main roof in the goaf, which is determined to be 15 m through field measurement; L_2 denotes the coal pillar width, of 20 m in this case; and L_3 denotes the extended length of 8.5 m through calculation. Through the width consideration of the air return way of 5 m, the position of the main roof fracturing was approximately 3.5 m inside the coal.

4. Similar Simulation Testing and Detection of Ultra-Thick Hard Sandstone Roof Fracture

In order to obtain the fracturing position and fracturing characteristics of the roof for 11215 working face under the neighboring goaf influence, similar simulation testing was adopted to conduct research, as well as the fracturing position

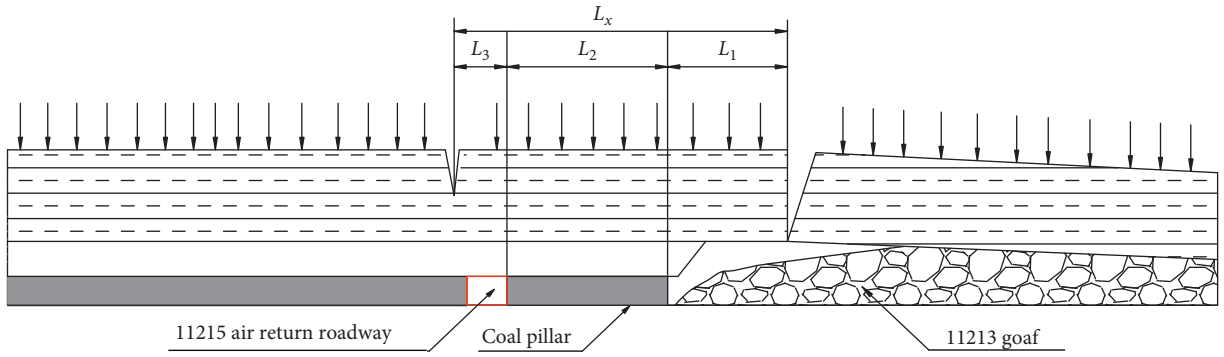

Figure 8: Main roof suspension state above the coal pillar after No. 11213 working face.

detection of the roof at the side of goaf in combination with the hole-drilling method for mutual verification.

A two-dimensional areal model was utilized as the physical model. The scheme was the process simulation of the first mining influence, produced by 11213 working face mining, and the second mining, produced by the 11215 working face mining, on 11215 air return way. Based on the geological conditions and similarity parameters, the model basic parameters were obtained and are presented in Table 2.

From Figure 9, it could be observed that subsequent to the 11215 working face mining, due to the influence of 11213 goaf, the immediate roof sustained caving and contacted the bottom plate. At 34 m above the coal bed, apparent roof bedding separation occurred, with significant fracture development and the maximum height of fracture development reached up to approximately 256 m. At this time frame, the fracturing angle at the left side above the coal pillar was 74°, and the hanging arch distance of immediate roof was 1.9 m, and for 20 m overlying rock, it was 7.5 m. The fracturing angle at the right side was 58°, the hanging arch distance of immediate roof was 4.4 m, and for the 20 m overlying rock, it was 17 m. Since the 11215 working face excavated, the displacement of overlying strata is very large, which reached up to 5900 mm (Figure 10).

In order to further prove the suspension state of the roof in the neighboring goaf, the tunnel detection and the drilling method was used. The boreholes were drilled from the 11215 air return way to the side of 11213 goaf. When the 11215 working face advanced to the influence sphere of 11213 goaf, a group of fan-shaped boreholes was drilled into the 11215 air return way, as aforementioned. The drill site position is presented in Figure 11, in which, the drill site was 518 m from the 11213 open-off cut and 89m ahead of the 11215 working face.

The specific construction location of three detection holes is as follows: the roadway sides of coal pillar in the air return way of 11215 working face were 0.72 m, 0.1 m, and 0.1 m from the roof. The field construction parameters are presented in Table 3, and the site construction scheme is presented in Figure 12.

Table 3 and Figure 12 present the hanging arch length L of the initial roof and the boundary line for the roof fracture and the fracturing angle; the following could be observed:

Table 2: Basic parameter table for physical similarity model.

Item	Parameters	Item	Parameters
Model type	2D pane	Excavation height	1.5 cm
Model length	2.5 m	Excavation distance	2.0 m
Model thickness	0.3 m	Model boundary	25 cm
Model height	127.3 cm	Excavation steps	50
Height of coal seam	1.5 cm	Single excavation distance	4 cm
Geometric similarity ratio	300 : 1	Excavation interval	0.5 h
Volume-weight ratio	1.667 : 1	Excavation time	25 h
Stress ratio	501 : 1	Upper load	0

(1) The overlying rock, detected at 32 m of altitude range above the coal pillar in the 11215 air return way was fine and the medium-grained sandstone. And, the stratification was not apparent, and the integrity was relatively good.

(2) The overlying rock, detected at the 32 m altitude range above the coal pillar in the 11215 air return way, had suspended roof structure in the 11213 goaf. The length of the hanging arch, detected through three boreholes, was 9.5 m, 11.6 m, and 14.1 m.

(3) The detected fracturing lines of roof are presented in Figure 9. The line formed by linking points A, B, and C was initially regarded as boundary line of the roof fracturing, in which, the fracturing line was 71°.

5. Fracture Stress Evolution of Ultra-Thick Hard Sandstone Roof

According to geological conditions in the 11215 working face, the UDEC was utilized to conduct research on the fracture stress evolution of roof in the inclined direction of the 11215 working face. The mechanical parameters of coal/rock mass and their contact surfaces adopted in numerical simulation are given in Tables 4 and 5. Following the 11213 working face mining, the overlying rock fracture is presented in Figure 13(a). The detection lines were arranged on the main roof of 20 m in thickness, while its stress variation curves were obtained, as presented in

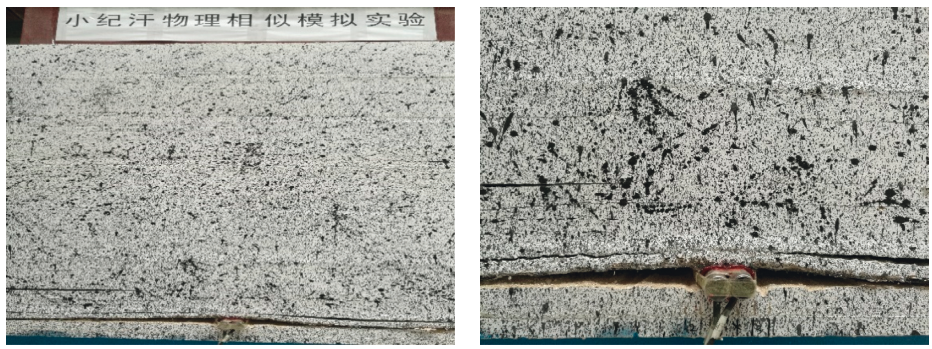

(a) (b)

Figure 9: Development figures of roof cracks in No. 11215 working face: the Chinese characters in (a) mean "physical similarity simulation test of Xiaojihan coal mine".

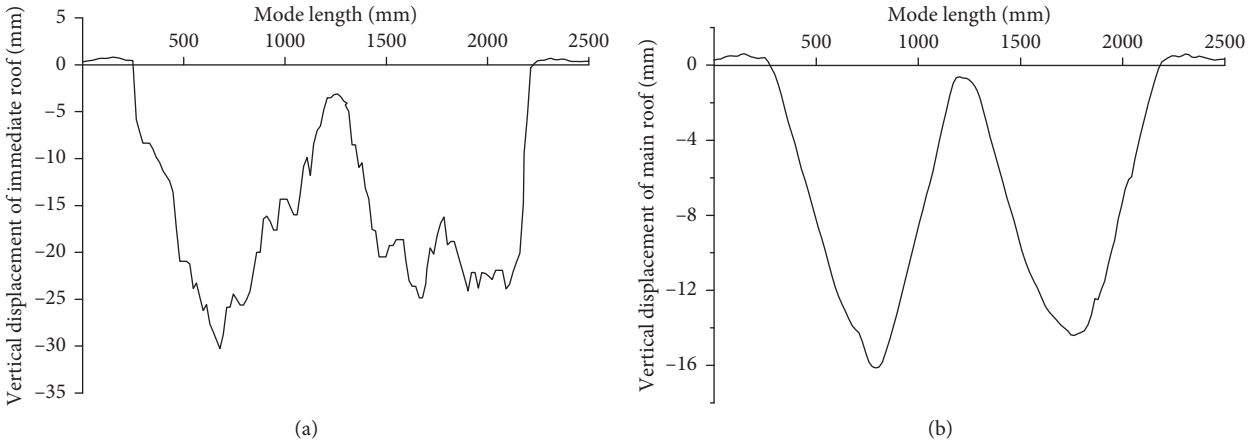

(a) (b)

Figure 10: Rock movement characteristics during excavation of working face: (a) the sinking curve of immediate roof; (b) the sinking curve of main roof.

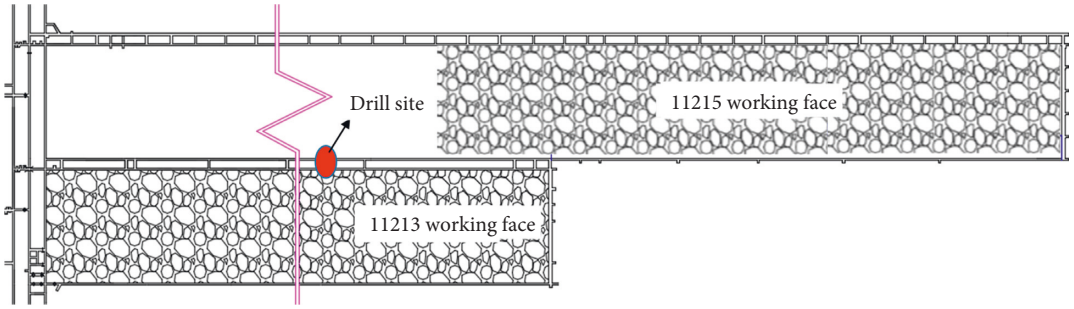

Figure 11: Location map of No. 11215 working face.

Table 3: Construction parameters of borehole detection.

Number	Elevation angle	Horizontal angle	Hole depth (m)	Aperture (mm)	Distance (m)	Distance from the roof (m)
1	29	0	45	93		0.72
2	35	0	40.5	93	1	0.1
3	40	0	50	93		0.1

Figure 13(c). Regarding the stress of the 11215 working face, the closer the distance to the 11213 working face was, the higher the stress of the main roof was, for which, the maximum occurred at 10 m on the left side of the air return roadway. Under the influence of air return roadway, the stress variation displayed hump shape. In the middle part of

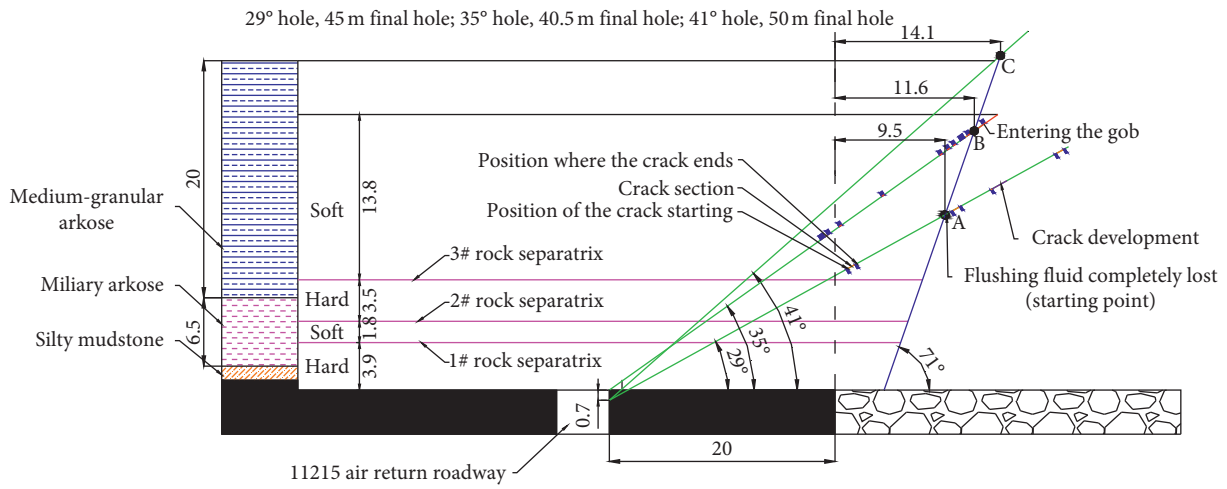

Figure 12: Lateral suspension roof shape detection hole above the coal pillar of the 11215 return airway.

Table 4: Mechanical parameters of coal and rock mass in numerical model.

Rock type	Thickness (m)	Density (KN/m^3)	Elastic module (GPa)	Poisson's ratio	Cohesion (MPa)	Fractional angle (°)
Mudstone	6	18	9.8	0.32	1.4	20
Sandstone	14	22	15	0.28	11.4	23
Mudstone	12	19	10.2	0.32	1.4	20
Fine sandstone	12	20	16	0.29	5.9	30
Mudstone	3	19	10.2	0.32	1.4	20
Siltite	7	21	14.4	0.29	10.2	31
Mudstone	5	19	9.6	0.32	1.4	19
Medium-grained stone	23	26	15.2	0.30	7.9	30
Siltite	8	23	14.4	0.29	10.2	29
Medium-grained stone	19.8	25	15.2	0.33	7.9	31
Fine sandstone	7	23	16	0.33	5.9	31
Coal	4.5	14	2.2	0.30	4.8	13
Mudstone	3	18	9.8	0.32	1.4	20
Sandstone	11	24	14.2	0.28	11.0	23

Table 5: Mechanical parameters of contact surface of strata in the model.

Rock type	Normal stiffness (GPa)	Shear stiffness (GPa)	Cohesion (MPa)	Frictional angle (°)	Tensile strength (MPa)
Mudstone	1.0	2.2	0	10	0
Sandstone	2.6	5.8	0	22	0
Mudstone	0.8	2.0	0	10	0
Fine sandstone	3.5	7.4	0	23	0
Mudstone	0.8	2.2	0	10	0
Siltite	3.4	7.0	0	22	0
Mudstone	1.0	2.2	0	12	0
Medium-grained stone	3.6	7.4	0	22	0
Siltite	3.4	7.0	0	20	0
Medium-grained stone	3.6	7.4	0	22	0
Fine sandstone	3.5	7.0	0	23	0
Coal	0.5	2.0	0	16	0
Mudstone	1.0	2.2	0	12	0
Sandstone	3.2	6.8	0	22	0

coal pillar, the stress reached up to the maximum of 14.55 MPa.

Subsequent to the 11213 working face excavation completion, the 11215 working face excavation was carried out. Similarly, the detection lines were arranged on the main roof, while its stress variation curves were obtained, as presented in Figure 13(d). Following the 11215 working face excavation, the overlying rock stress in the main roof was basically zero. Also, the stress in the middle part of the working face was higher was 13.5 MPa. Due to the goaf influence in the 11213 working face, the stress above the coal pillar first increased and consequently decreased. Near the

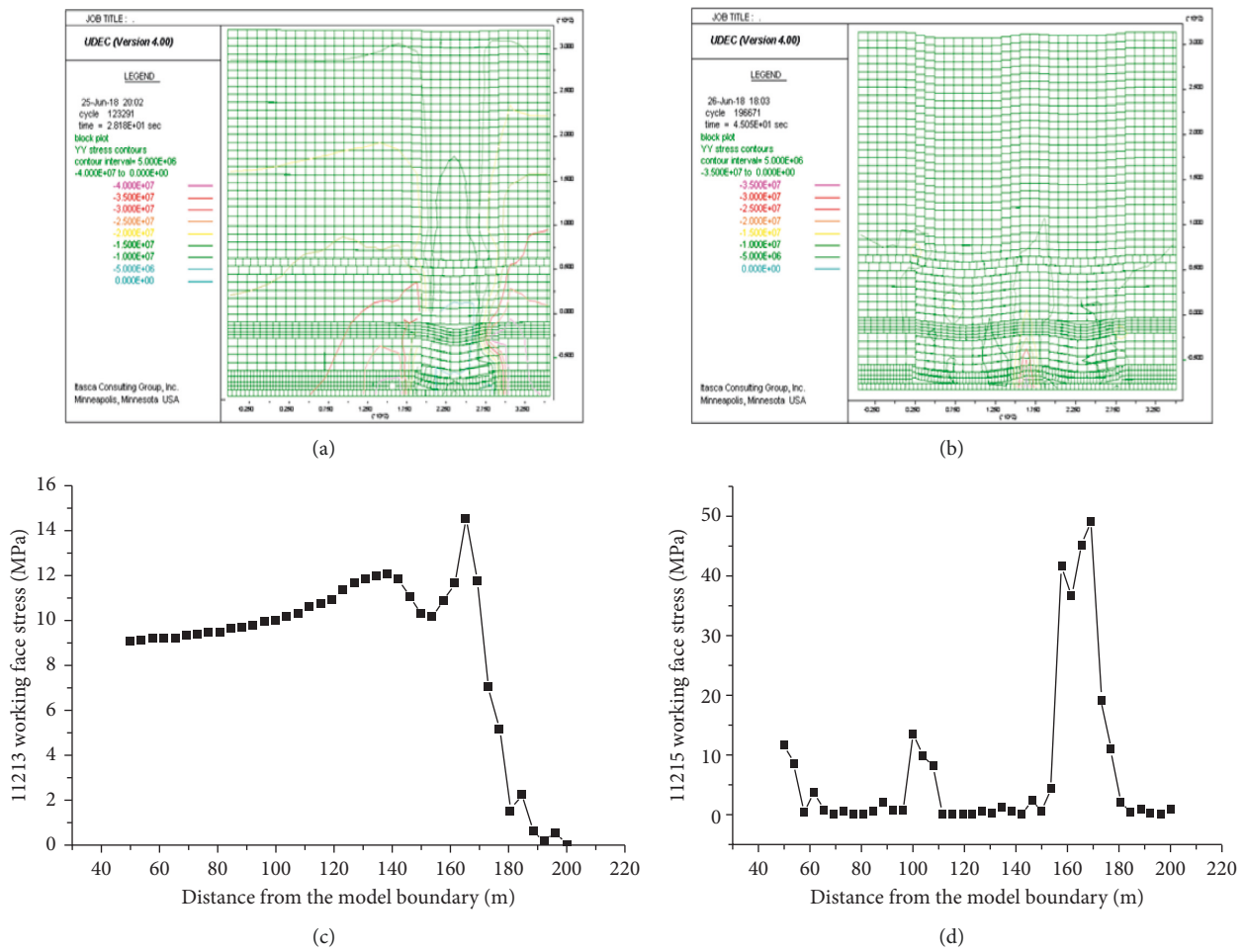

Figure 13: Roof breaking and stress evolution: (a) 11213 working face excavation; (b) 11215 working face excavation; (c) stress distribution of the 11213 working face excavation; (d) stress distribution of the 11215 working face excavation.

position of 5 m from the goaf of the 11213 working face, the stress reached the maximum of 49.1 MPa.

6. Conclusions

(1) Through field measurement and laboratory test analysis, it was discovered that the roof of 11215 working face in Xiaojihan coal mine belonged to the interbedding of sandstone and mudstone as a whole, in which, the sandstone played a main role. The roof strata had good integrity, lower porosity, and high density. The main roof was 19.79 m feldspar sandstone stratum (nearly 20 m ultra-thick sandstone).

(2) The working face side was simplified to "cantilever-simply supported" beam structure. The force situation of fractured stratum on the roof was analyzed through the elastic foundation beam model. According to calculation results, it could be obtained that the fracturing line of the main roof in 11215 working face was approximately 3.5 m within the coal.

(3) Through the methods combination of similar simulations and field measurements of drilled holes, the hanging arch lengths in the goaf of 6.4 m, 22.1 m, and 29.6 m, high above the coal bed, were determined to be 9.5 m, 11.6 m, and 14.1 m, respectively. Furthermore, the fracturing angle of the main roof was determined to be 71° through the same method combination.

(4) The overlying rock fracture and stress evolution laws above the coal pillar prior to and following mining of 11215 working face under the influence of 11213 goaf were simulated through the UDEC numerical simulation method. The simulation results demonstrated that the 11215 working face was highly influenced by the 11213 goaf, whereas its lateral supporting stress reached the maximum at the position of 5 m from 11213 goaf, consequently having a significant influence on the roadway deformation.

Data Availability

The data used to support the findings of this study are included and shown within the article.

Conflicts of Interest

The authors declare that there are no conflicts of interest regarding the publication of this paper.

Acknowledgments

The work presented in this paper was funded by the general program of the National Natural Science Fund project in China (No. 51674241).

References

[1] China Coal Industry Association, *Annual report on the development of Chinese coal industry in 2017*, China Coal Industry Association, Beijing, China, 2017.

[2] C. L. Han, N. Zhang, B. Y. Li, G. Y. Si, and X. G. Zheng, "Pressure relief and structure stability mechanism of hard roof for gob-side entry retaining," *Journal of Central South University*, vol. 22, no. 11, pp. 4445–4455, 2015.

[3] J. He, L. M. Dou, A. Y. Cao, S. Y. Gong, and J. W. Lu, "Rock burst induced by roof breakage and its prevention," *Journal of Central South University of Technology*, vol. 19, no. 4, pp. 1086–1091, 2012.

[4] W. L. Shen, J. B. Bai, X. Y. Wang, and Y. Yu, "Response and control technology for entry loaded by mining abutment stress of a thick hard roof," *International Journal of Rock Mechanics and Mining Sciences*, vol. 90, pp. 26–34, 2016.

[5] T. B. Zhao, Y. C. Yin, and Y. L. Tan, "Safe mining and new prediction model in coal seam with rock burst induced by roof," *Disaster Advances*, vol. 5, no. 4, pp. 961–965, 2012.

[6] Q. S. Bai, S. H. Tu, F. T. Wang, and C. Zhang, "Field and numerical investigations of gateroad system failure induced by hard roofs in a longwall top coal caving face," *International Journal of Coal Geology*, vol. 173, pp. 176–199, 2017.

[7] J. Guo, G. R. Feng, P. F. Wang, T. Y. Qi, X. R. Zhang, and Y. G. Yan, "Roof strata behavior and support resistance determination for ultra-thick longwall top coal caving panel: a case study of the Tashan coal mine," *Energies*, vol. 11, no. 5, 2018.

[8] W. B. Guo, H. S. Wang, G. W. Dong, L. Li, and Y. G. Huang, "A case study of effective support working resistance and roof support technology in thick seam fully-mechanized face mining with hard roof conditions," *Sustainability*, vol. 9, no. 6, 2017.

[9] J. L. Jia, L. W. Cao, D. J. Zhang et al., "Study on the fracture characteristics of thick-hard limestone roof and its controlling technique," *Environmental Earth Sciences*, vol. 76, no. 17, 2017.

[10] J. G. Ning, J. Wang, L. S. Jiang, N. Jiang, X. S. Liu, and J. Q. Jiang, "Fracture analysis of double-layer hard and thick roof and the controlling effect on strata behavior: a case study," *Engineering Failure Analysis*, vol. 81, pp. 117–134, 2017.

[11] Y. M. Shu and Y. L. Liu, "The mechanism analysis of rock burst in Xinxing mine," in *Proceedings of 4th International Conference on Energy and Environmental Protection*, pp. 528–531, Shenzhen, China, December 2015.

[12] W. Wang, Y. P. Cheng, H. F. Wang et al., "Fracture failure analysis of hard-thick sandstone roof and its controlling effect on gas emission in underground ultra-thick coal extraction," *Engineering Failure Analysis*, vol. 54, pp. 150–162, 2015.

[13] X. L. Li, C. W. Liu, Y. Liu, and H. Xie, "The breaking span of thick and hard roof based on the thick plate theory and strain energy distribution characteristics of coal seam and its application," *Mathematical Problems in Engineering*, vol. 2018, pp. 1–14, 2017.

[14] T. Zhao, C. Y. Liu, K. Yetilmezsoy, B. S. Zhang, and S. Zhang, "Fractural structure of thick hard roof stratum using long beam theory and numerical modeling," *Environmental Earth Sciences*, vol. 76, no. 21, 2017.

[15] W. Wang, Y. P. Cheng, H. F. Wang, W. Li, and L. Wang, "Coupled disaster-causing mechanisms of strata pressure behavior and abnormal gas emissions in underground coal extraction," *Environmental Earth Sciences*, vol. 74, no. 9, pp. 6717–6735, 2015.

[16] Q. S. Wu, L. S. Jiang, Q. L. Wu, Y. C. Xue, and B. Gong, "A study on the law of overlying strata migration and separation space evolution under hard and thick strata in underground coal mining by similar simulation," *Dyna Ingenieria e Industria*, vol. 94, no. 1, pp. 175–181, 2018.

[17] C. P. Lu, L. M. Dou, N. Zhang et al., "Microseismic frequency-spectrum evolutionary rule of rockburst triggered by roof fall," *International Journal of Rock Mechanics and Mining Sciences*, vol. 64, pp. 6–16, 2013.

[18] C. P. Lu, Y. Liu, H. Y. Wang, and P. F. Liu, "Microseismic signals of double-layer hard and thick igneous strata separation and fracturing," *International Journal of Coal Geology*, vol. 160-161, pp. 28–41, 2016.

[19] Z. X. Yu, F. X. Jiang, Q. J. Zhu, and S. T. Zhu, *Study on Stability of Thick-Hard Key Stratum Based on Numerical Simulation in Longwall Mining*, 2014.

[20] C. Xu, L. Yuan, Y. P. Cheng, K. Wang, A. T. Zhou, and L. Y. Shu, "Square-form structure failure model of mining-affected hard rock strata: theoretical derivation, application and verification," *Environmental Earth Sciences*, vol. 75, no. 16, 2016.

[21] H. He, L. M. Dou, J. Fan, T. T. Du, and X. L. Sun, "Deep-hole directional fracturing of thick hard roof for rockburst prevention," *Tunnelling and Underground Space Technology*, vol. 32, pp. 34–43, 2012.

[22] Z. T. Zheng, Y. Xu, D. S. Li, and J. H. Dong, "Numerical analysis and experimental study of hard roofs in fully mechanized mining faces under sleeve fracturing," *Minerals*, vol. 5, no. 4, pp. 758–777, 2015.